Science of the Total Environment 871 (2023) 161830

Contents lists available at ScienceDirect

Science of the Total Environment

journal homepage: www.elsevier.com/locate/scitotenv

Levels and distribution profiles of Per- and Polyfluoroalkyl Substances (PFAS) in a high Arctic Svalbard ice core

William F. Hartz [a,b,*], Maria K. Björnsdotter [c,d], Leo W.Y. Yeung [d], Andrew Hodson [b,e], Elizabeth R. Thomas [f], Jack D. Humby [f], Chris Day [a], Ingrid Ericson Jogsten [d], Anna Kärrman [d], Roland Kallenborn [g,h]

[a] Department of Earth Sciences, University of Oxford, South Parks Road, Oxford OX1 3AN, United Kingdom
[b] Department of Arctic Geology, University Centre in Svalbard (UNIS), NO-9171, Longyearbyen, Svalbard, Norway
[c] Institute of Environmental Assessment and Water Research (IDAEA-CSIC), C/Jordi Girona, 18-26, 08034 Barcelona, Catalonia, Spain
[d] Man-Technology-Environment Research Centre (MTM), Örebro University, SE-701 82 Örebro, Sweden
[e] Department of Environmental Sciences, Western Norway University of Applied Sciences, NO-6851 Sogndal, Norway
[f] Ice Dynamics and Paleoclimate, British Antarctic Survey, High Cross, Cambridge CB3 0ET, United Kingdom
[g] Faculty of Chemistry, Biotechnology and Food Sciences (KBM), Norwegian University of Life Sciences (NMBU), NO-1432 Ås, Norway
[h] Department of Arctic Technology, University Centre in Svalbard (UNIS), NO-9171, Longyearbyen, Svalbard, Norway

HIGHLIGHTS

- 26 PFAS were detected in a remote Arctic ice core from Svalbard
- FTOHs, as well as HFCs and other CFC replacement products, provide an atmospheric precursor source to PFCAs
- TFA represented 71 % of the total mass of $C_2 - C_{11}$ PFCAs, and its atmospheric deposition is increasing
- Structural isomers of PFOS suggest an ECF manufacturing source
- TFA and PFOS were found to be mobile during meltwater percolation

GRAPHICAL ABSTRACT

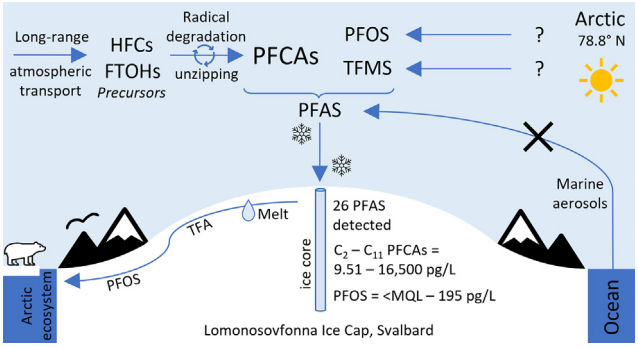

ARTICLE INFO

Editor: Jay Gan

Keywords:
Temporal trends
Trifluoroacetic acid
Fluorotelomer alcohols
Hydrofluorocarbons
Long-range transport
Snowmelt

ABSTRACT

Per- and polyfluoroalkyl substances (PFAS) are a group of persistent organic contaminants of which some are toxic and bioaccumulative. Several PFAS can be formed from the atmospheric degradation of precursors such as fluorotelomer alcohols (FTOHs) as well as hydrochlorofluorocarbons (HFCs) and other ozone-depleting chlorofluorocarbon (CFC) replacement compounds. Svalbard ice cores have been shown to provide a valuable record of long-range atmospheric transport of contaminants to the Arctic. This study uses a 12.3 m ice core from the remote Lomonosovfonna ice cap on Svalbard to understand the atmospheric deposition of PFAS in the Arctic. A total of 45 PFAS were targeted, of which 26 were detected, using supercritical fluid chromatography (SFC) tandem mass spectrometry (MS/MS) and ultra-performance liquid chromatography (UPLC) MS/MS. C_2 to C_{11} perfluoroalkyl carboxylic acids (PFCAs) were detected continuously in the ice core and their fluxes ranged from 2.5 to 8200 ng m^{-2} yr^{-1} (9.51–16,500 pg L^{-1}). Trifluoroacetic acid (TFA) represented 71 % of the total mass of $C_2 - C_{11}$ PFCAs in the ice core and had increasing temporal trends in deposition. The distribution profile of PFCAs suggested that FTOHs were likely the atmospheric precursor to $C_8 - C_{11}$ PFCAs, whereas $C_2 - C_6$ PFCAs had alternative sources, such as HFCs and other CFC replacement compounds. Perfluorooctanesulfonic acid (PFOS) was also widely detected in 82 % of ice core subsections, and its isomer profile (81 % linear) indicated an electrochemical fluorination manufacturing source. Comparisons of PFAS concentrations with a marine aerosol proxy showed that marine aerosols were insignificant for the deposition of

* Corresponding author at: Department of Earth Sciences, University of Oxford, South Parks Road, Oxford OX1 3AN, United Kingdom.
E-mail address: william.hartz@earth.ox.ac.uk (W.F. Hartz).

http://dx.doi.org/10.1016/j.scitotenv.2023.161830
Received 4 November 2022; Received in revised form 20 January 2023; Accepted 21 January 2023
Available online 28 January 2023

PFAS on Lomonosovfonna. Comparisons with a melt proxy showed that TFA and PFOS were mobile during meltwater percolation. This indicates that seasonal snowmelt and runoff from post-industrial accumulation on glaciers could be a significant seasonal source of PFAS to ecosystems in Arctic fjords.

1. Introduction

Per- and polyfluoroalkyl substances (PFAS) are a diverse group of organofluorine compounds, used in a variety of industrial and consumer applications (Wang et al., 2021). However, many PFAS are persistent, toxic and bioaccumulative (Frömel and Knepper, 2010; Conder et al., 2008; Jensen and Leffers, 2008). Research has been particularly focused on perfluoroalkyl acids (PFAAs), including perfluoroalkyl carboxylic acids (PFCAs) and perfluoroalkyl sulfonic acids (PFSAs). The ubiquitous detection of PFAAs and other PFAS in the environment, including Arctic biota and abiota confirms the high environmental mobility of PFAS (Muir et al., 2019).

The low volatility and high solubility of PFCAs and PFSAs (present in the environment largely in their deprotonated forms) do not promote direct long-range atmospheric transport from industrialized or populated areas to remote regions, such as the Arctic (Rayne and Forest, 2009). However, several mechanisms for long-range transport of PFAS to the Arctic have been proposed and investigated. One such mechanism is through long-range ocean currents, whereby ocean currents distribute PFAS from source regions to remote Arctic marine environments (Benskin et al., 2012; Yeung et al., 2017). Marine aerosols have also been identified as PFAS carriers for long-range transport (Sha et al., 2022). The long-range atmospheric transport of volatile precursor PFAS, followed by their atmospheric degradation to PFAAs and subsequent deposition has also been identified (Ellis et al., 2004; Young et al., 2007). However, the relative significance of each transport mechanism remains unclear.

Several volatile neutral PFAS have been identified as atmospheric precursors to PFAS degradation products. These include fluorotelomer alcohols (FTOHs), N-alkylated perfluoroalkane sulfonamides (FASAs), perfluoroalkane sulfonamido ethanols (FASEs), and fluorotelomer acrylates (FTAs), several of which have been identified in the Arctic atmosphere, including in Svalbard (Norwegian Arctic) (Cai et al., 2012; Dreyer et al., 2009; Shoeib et al., 2006; Stock et al., 2007; Xie et al., 2015). These studies found FTOHs dominated the mass of precursors detected and that the most abundant precursor targeted was 8:2 FTOH.

Several studies have undertaken laboratory experiments to investigate the atmospheric chemistry of precursors including FTOHs (Ellis et al., 2004; Sulbaek Andersen et al., 2005), FASAs (Martin et al., 2006), FASEs (D'eon et al., 2006), and FTAs (Butt et al., 2009). All these studies found that these precursors would be able to degrade via a gaseous radical-mediated process to a suite of equal or shorter chain (protonated) PFCAs aided by an unzipping cycle. Once PFAAs have formed in the atmosphere, they will be effectively scavenged by wet deposition (Wang et al., 2019). Hence during precipitation, the vast majority of PFAAs will be removed from the atmosphere and undergo deposition (in their deprotonated form) (Taniyasu et al., 2013; Pike et al., 2021).

Whilst trifluoroacetic acid (TFA) and shorter chain PFAAs can form from the degradation of longer chain precursors such as FTOHs (Ellis et al., 2004), these short-chain PFAAs can have additional and more significant atmospheric precursors. For example, hydrofluorocarbons (HFCs) (Young et al., 2009a), hydrochlorofluorocarbons (HCFCs) (Wallington et al., 1994), hydrofluoroethers (HFEs) (Oyaro et al., 2005), and hydrofluoroolefins (HFOs) (Young et al., 2009b), have been identified as atmospheric precursors to TFA and other short-chain PFAAs. HFCs, HCFCs, HFEs, and HFOs were introduced as replacement products for ozone-depleting chlorofluorocarbons (CFCs) in the 1990s. CFCs were previously used as cooling agents but were banned in 1989 after the introduction of the Montreal protocol (Velders et al., 2007). However, TFA has been found ubiquitously in surface snow, including in the Arctic (Björnsdotter et al., 2021), and environmental levels are increasing (Pickard et al., 2020; Freeling et al., 2022). Trifluoromethanesulfonic acid (TFMS) was also recently detected ubiquitously in surface snow in the Arctic, however, the study was not able to assign a source (Björnsdotter et al., 2021).

Ice cores can provide a record of several years of snow accumulation and hence a route to understanding PFAS atmospheric sources and transformation processes. Remote ice cores spanning several years have already been used to elucidate atmospheric sources of PFAS on the Devon Ice Cap and Mt. Oxford icefield in the Canadian Arctic (Pickard et al., 2020; Pickard et al., 2018). Unlike long-term atmospheric monitoring studies, ice cores can help to retrospectively investigate atmospheric processes and deposition. Svalbard (Norwegian Arctic) is known to receive contaminated air masses from Eurasia and has several established sites for ice core research (Garmash et al., 2013; Isaksson et al., 2003). Lomonosovfonna is the highest elevation ice cap (1198 m.a.s.l.) in the Svalbard Archipelago and is sufficiently remote and high elevation to capture predominantly long-range processes (Garmash et al., 2013; Osmont et al., 2018). A study of 22 sites on Svalbard glaciers identified Lomonosovfonna as an optimal site to investigate long-range pollution deposition (Barbaro et al., 2021). As observed elsewhere in the Arctic, local sources of PFAS have also been identified in Svalbard, including firefighting training and landfill sites in Longyearbyen and Ny-Ålesund (Kwok et al., 2013a; Skaar et al., 2019; Ali et al., 2021).

This study uses a 12.3 m ice core (spanning 2006 to 2019) from Lomonosovfonna to investigate the long-range atmospheric deposition of PFAS to the Arctic. By targeting 45 different PFAS analytes, this study aims to understand the sources and processes for PFAS deposition on Lomonosovfonna. This study (i) compares annual PFAS fluxes with other remote Arctic ice cores, (ii) elucidates PFAS precursor sources or otherwise (iii) compares PFAS concentrations with a marine aerosol proxy, (iv) investigates air mass source regions, and (v) investigates the redistribution of PFAS during meltwater percolation. To the best of our knowledge, this work reports the first remote ice core in the European Arctic to be analyzed for neutral and ultra-short chain PFAS, as well as several other PFAS.

2. Materials and methods

2.1. Ice core drilling and dating

In April 2019, a 12.3 m ice core (2006–2019), diameter 14.0 cm, was drilled on Lomonosovfonna (78°49.454′N, 17°26.193′E, 1198 m.a.s.l., Fig. 1) using a Kovacs Mark V core barrel and SideWinder (Kovacs Enterprise, LLC, Roseburg, OR, USA). The ice core was transported to the University Centre in Svalbard (UNIS) in Longyearbyen by snowmobile and stored at −20 °C prior to analysis. Further information on the characteristics of the site is described in the supporting information (page S1).

2.2. Sample preparation and PFAS analysis

A total of 45 different PFAS analytes were targeted as follows. PFAAs targeted were C_2 – C_{14}, C_{16}, and C_{18} PFCAs, and C_1 – C_{10} and C_{12} PFSAs. Fluorotelomers targeted were 4:2 FTSA, 6:2 FTSA, 8:2 FTSA, 6:2 FTUCA and 8:2 FTUCA. Further anionic target analytes included 6:2 Cl-PFESA, 8:2 Cl-PFESA, HFPO-DA (GenX), and ADONA. In total, 9 neutral compounds were also targeted: FBSA, MeFBSA, FHxSA, MeFHxSA, FOSA, MeFOSA, EtFOSA, MeFOSE and EtFOSE. C_2 – C_3 PFCAs and C_1 – C_3 PFSAs were measured by supercritical fluid chromatography (SFC) tandem mass spectrometry (MS/MS) system. All other compounds were measured by ultra-performance liquid chromatography (UPLC) MS/MS. The

Fig. 1. Map showing the location of the Lomonosovfonna ice core drilling site. Insert: Location of Svalbard in the northern hemisphere. The map was reproduced from TopoSvalbard, Norwegian Polar Institute.

quantification of branched isomers of PFOS and PFHxS is described in the supporting information (pages S4 – S5). A full list of names, abbreviations and instrument methods are described in Table S1.

In the cold lab at UNIS (−20 °C), the outer surfaces of the ice core (1.0–2.3 cm) were carefully removed and discarded to avoid possible contamination from drilling, handling, transport, and storage. Subsamples for water stable isotopes and major ions were collected at a 5 cm resolution. Subsections for PFAS analysis (n = 17) were sampled sequentially, such that each section was at least 2 kg, into sterile polyethylene whirltop bags, which were then stored frozen at −20 °C. Immediately prior to extraction, ice core samples were melted and bottled into precleaned polypropylene containers. Samples were extracted by weak anion exchange solid-phase extraction following the ISO25101 method with some modifications (ISO 25101:2009, 2009). Full details can be found in the supporting information (pages S1 – S9). This includes details on the chemicals and reagents, sample extraction, instrument analysis, quality control and quality assurance, MQLs (method quantification limits), Hybrid Single-Particle Lagrangian Integrated Trajectory model (HYSPLIT) analysis, major ion analysis and water stable isotope analysis.

2.3. Ice core dating and data treatment

An age-depth relationship for the ice core was established using a multi-proxy approach including (i) seasonal variations in the stable isotope ratio $\delta^{18}O$, (ii) seasonal variations in the $[Na^+]/[Cl^-]$ ratio, and (iii) a peak in non-sea-salt sulfate ($nssSO_4^{2-}$) at 404.5 cm water equivalent (weq) assigned to be the 2011 Grímsvötn volcanic eruption in Iceland (Burgay et al., 2021; Karasiński et al., 2014). As such, 12 complete annual layers were observed, and the annual layers were counted from 2019 back to 2006 ± 2 years (Fig. S1).

PFAS analyte concentrations are reported in pg L^{-1}. In order to remove the effects of annual accumulation variability (measured to be 26–75 cm weq for 2007–2018 from this ice core), annual flux values were also calculated. Analyte concentrations (in pg L^{-1}) were first converted into ng $year^{-1}$. This was then divided by the cross-sectional area of the ice core (0.0154 m^2) to give a flux value in ng m^{-2} yr^{-1}. The values for the Na^+ concentrations and melt proxy $\log([Na^+]/[Mg^{2+}])$ for each PFAS subsection of the ice core, were calculated by averaging across the 5 cm subsamples (n = 7–19 subsamples) contained within each of the PFAS subsections. Spearman rank correlation coefficients (r) were used to calculate correlations between various PFAS and Na^+/melt proxy values. Tests for statistical significance were performed using a two-tailed Student's t-test (p). Only those values with $p < 0.01$ were considered significant ($\alpha = 0.01$).

3. Results and discussion

3.1. Fluxes and concentrations of PFAS on Lomonosovfonna

In summary, all $C_2 – C_{11}$ PFCAs were detected continuously throughout the whole core which spanned 2006–2019 (n = 17). There was also widespread detection of FBSA, FOSA, PFHxS, and PFOS, as well as C_{12} and C_{13} PFCAs (which had detection frequencies >MQL in >50 % of core subsections). C_{14} and C_{15} PFCAs, PFBS, PFPeS, 6:2 FTSA, 6:2 FTUCA, 8:2 FTUCA and 5 neutral PFAS (MeFBSA, FHxSA, EtFOSA, MeFOSE and EtFOSE) were also detected, albeit with detection frequencies >MQL in <50 % of core subsections. For these compounds without continuous detection, there were no clear trends based on detection frequencies alone. However, PFOS and FBSA were both detected continuously from 2010 and 2011, respectively, to 2019. Trends in atmospheric deposition fluxes of $C_2 – C_{11}$ PFCAs, PFHxS and PFOS are discussed further in Section 3.4. C_{18} PFCA, six PFSAs (C_2, C_3, C_7, C_9, C_{10}, and C_{12}), 4:2 FTSA, 8:2 FTSA, PFECHS, 4 PFAS with ether functionality (6:2 Cl-PFESA, 8:2 Cl-PFESA, ADONA and HFPO-DA i.e. GenX) and 2 neutral PFAS (MeFHxSA and MeFOSA) were not detected throughout the entire core. Further information on detection, concentrations, and fluxes can be found in Tables S7 – S12.

For $C_2 – C_{11}$ PFCAs, fluxes ranged from 2.5 to 8200 ng m^{-2} yr^{-1} (9.51–16,500 pg L^{-1}). Fluxes of these PFCAs increased greatly towards shorter chain lengths (Fig. 2). Indeed, TFA represented 71 % of the mass of $C_2 – C_{11}$ PFCAs detected in the core. Longer chain lengths contributed significantly less mass: PFPrA (16 %), PFBA (6 %), PFPeA (2 %), PFHxA (1 %), PFHpA (1 %) and $C_8 – C_{11}$ PFCAs (each <1 %). Of the PFSAs targeted, only PFBS, PFPeS, PFHxS, and PFOS were detected. PFOS was the dominant PFSA, detected in 82 % of the subsections with fluxes ranging from 1.7 to 70 ng m^{-2} yr^{-1} (<MQL – 195 pg L^{-1}). PFHxS was detected in 65 % of the subsections and its fluxes ranged from 0.12 to 1.0 (<MQL – 28.3 pg L^{-1}). PFBS was detected in 24 % of the subsections (<MQL – 28.4 pg L^{-1}). 6:2 FTSA was also detected in 41 % of subsections (<MQL – 14.1 pg L^{-1}). Both 6:2 FTUCA and 8:2 FTUCA were detected in 35 % and 6 % of subsections, respectively (<MQL – 194 pg L^{-1}). Of the 9 targeted neutral compounds, 7 were detected. The most notable of these were FBSA and FOSA, which were detected in 82 % and 59 % of subsections.

Prior to this study, two other remote Arctic ice cores have been analyzed for PFAS. One of these is from the Devon Ice Cap in the Canadian Arctic in which 23 PFAS were analyzed including a range of PFCAs and PFSAs (Pickard et al., 2020; Pickard et al., 2018). The second is from the Mt. Oxford icefield in the Canadian Arctic which targeted $C_2 – C_4$ PFCAs (Pickard et al., 2020). Both the Devon Ice Cap and Lomonosovfonna ice cores had widespread detection of $C_2 – C_{11}$ PFCAs. An overview comparing the fluxes of $C_2 – C_{11}$ PFCAs and PFOS on Lomonosovfonna (2007–2018, this study), Devon Ice Cap (2007–2014) (Pickard et al., 2020; Pickard et al., 2018), and Mt. Oxford Ice Cap (2007–2016) (Pickard et al., 2020) can be seen in Fig. 2. For measurements below the limit of detection, fluxes were calculated using half the limit of detection (which was only for some

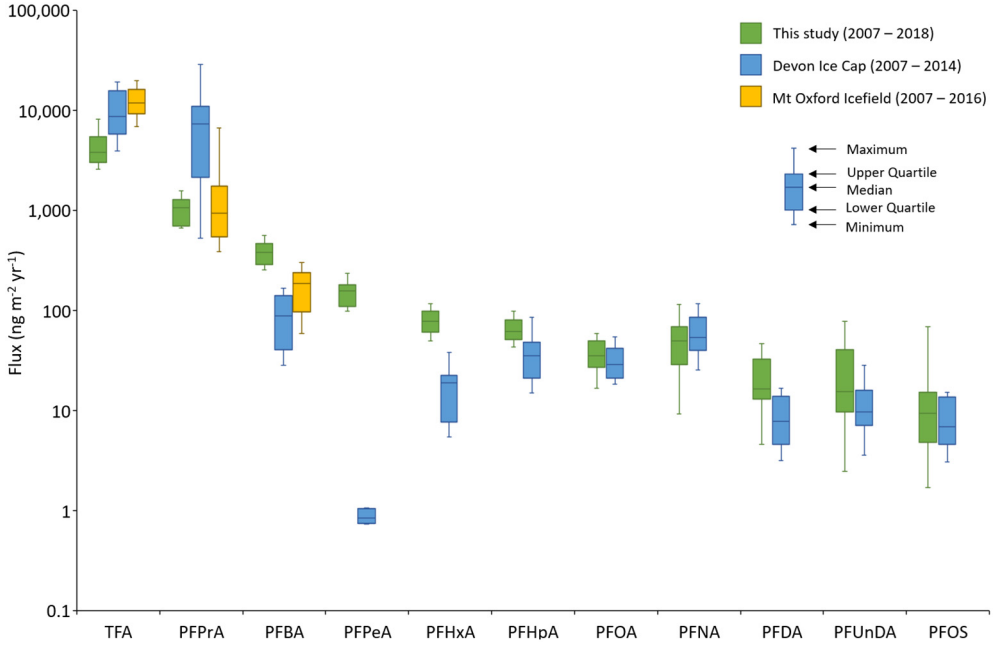

Fig. 2. Fluxes (ng m^{-2} yr^{-1}) of C_2 – C_{11} PFCAs and PFOS in Arctic ice cores from Lomonosovfonna (2007–2018, this study), Devon Ice Cap (2007–2014) (Pickard et al., 2020; Pickard et al., 2018) and the Mt. Oxford icefield (2007–2016) (Pickard et al., 2020).

measurements of PFOS on Lomonosovfonna and PFPeA on the Devon Ice Cap). Herein, the comparisons between fluxes and detection frequencies refer to these time periods. Another study measured PFAS in an ice core from the Longyearbreen glacier on Svalbard (Kwok et al., 2013b). However, owing to the proximity of this site to a number of significant PFAS sources in Longyearbyen settlement (4–10 km) (Skaar et al., 2019; Ali et al., 2021), it would be inappropriate to use this record to understand the background atmospheric processes of PFAS in the Arctic. Furthermore, Longyearbreen is not an established site for multiyear ice core records on Svalbard and its high equilibrium line altitude (~615 m.a.s.l. in 2004) casts doubt on the potential to retrieve reliable multiyear ice core records from this glacier (Yde et al., 2008).

The fluxes of TFA and PFPrA were typically lower on Lomonosovfonna compared to the Devon Ice Cap and Mt. Oxford icefield, whereas the fluxes of PFBA were higher. For C_5 – C_{11} PFCAs, measured only on the Devon Ice Cap, fluxes were similar or higher on Lomonosovfonna. C_5 – C_7 PFCAs were higher on Lomonosovfonna – fluxes of PFPeA, PFHxA, and PFHpA were on average 56, 4.6 and 1.6 times greater. The fluxes of PFDA and PFUnDA were also 2.3 and 2.0 times higher on Lomonosovfonna compared to the Devon Ice Cap. PFDoDA and PFTrDA were detected much more frequently in the Lomonosovfonna ice core (82 % and 88 %, respectively) compared to the Devon Ice Cap core (13 % and 0 %, respectively), despite similar detection limits around 2–4 pg L^{-1} for both ice cores. In contrast, the cores have similar fluxes of PFOA, PFNA and PFOS. United States Environmental Protection Agency (EPA) drinking water health advisory levels were consistently exceeded for both ice cores for PFOA, and sometimes exceeded for PFOS, despite their remote Arctic locations (Cousins et al., 2022).

FOSA fluxes remained low with 0.37–4.6 ng m^{-2} yr^{-1} (<MQL – 9.56 pg L^{-1}) on Lomonosovfonna and < MQL – 2.97 ng m^{-2} yr^{-1} (<MQL – 1.5 pg L^{-1}) on the Devon Ice Cap. This is most likely as a result of the phasing out of the production of perfluorooctane sulfonyl fluoride (POSF) by 3 M between 2000 and 2002 (Pickard et al., 2018).

The variability in fluxes between the three sites might be explained by the differences in each site's proximity to various sources and/or the differences in seasonal variations in accumulation on these glaciers. It is known that the deposition of some PFAAs in the Arctic is highly seasonal, with increased deposition during summer months (24-hour daylight) when atmospheric levels of hydroxyl (OH) radicals are higher (Björnsdotter et al., 2021; Wallington et al., 2006). Hence, increased accumulation in the winter months might underrepresent the relative atmospheric levels of some PFAAs. Indeed on Svalbard, precipitation is known to be greater during September – February, i.e. months with complete or partial darkness (Wickström et al., 2020).

3.2. Chemical sources of PFCAs to Lomonosovfonna

Several laboratory-based studies have identified volatile neutral PFAS, such as FTOHs, FASEs, FASAs, and FTAs to act as precursors and undergo a radical-mediated degradation to PFCAs (Ellis et al., 2004; Sulbaek Andersen et al., 2005; Martin et al., 2006; D'eon et al., 2006; Butt et al., 2009). These precursors are widespread in the Arctic atmosphere, with 8:2 FTOH being the dominant precursor (Cai et al., 2012; Dreyer et al., 2009; Shoeib et al., 2006; Stock et al., 2007; Xie et al., 2015). According to the study by Ellis et al. (Ellis et al., 2004), the radical-mediated degradation of 8:2 FTOH should result in approximately equal molar quantities of PFOA and PFNA (0.95:1 molar ratio) (Ellis et al., 2004). This may vary depending on the radical species present in the atmosphere and due to the presence of NO_x species. Nonetheless, the correlations between 45 pairs of PFCAs from TFA (C_2) – PFUnDA (C_{11}) were calculated (Table 1), since all these PFCAs were detected continuously in the ice core. All C_3 – C_6 PFCAs were significantly correlated ($r > 0.87$, $p < 0.01$) and sequential pairs of C_7 – C_{11} PFCAs were also significantly correlated ($r > 0.69$, $p < 0.01$). TFA (C_2) was not significantly correlated with any other PFCA ($r < 0.52$, $p > 0.03$). These results suggest a distinct division between TFA (C_2), C_3 – C_6, and C_7 – C_{11} PFCA sources.

As done previously for Arctic ice cores and snow pits, molar concentration ratios for even-odd PFCA homologues (MacInnis et al., 2017), TFA:PFPrA, PFBA:PFPeA, PFHxA:PFHpA, PFOA:PFNA, and PFDA:PFUnDA, were calculated, as these would be expected to be roughly equal if the major precursor was 2:2 FTOH, 4:2 FTOH, 6:2 FTOH, 8:2 FTOH, and 10:2 FTOH, respectively (Fig. 3). 82–94 % of the molar concentration ratios of PFHxA:PFHpA, PFOA:PFNA, PFDA:PFUnDA were between 0.5 and 2 (i.e. within a factor of 2). Given that, of these pairs, only PFOA and PFNA ($r = 0.77$, $p < 0.01$), and PFDA and PFUnDA ($r = 0.89$, $p < 0.01$), were significantly correlated, this suggests that C_8 – C_{11} PFCAs were mostly formed from the atmospheric degradation of 8:2 FTOH and 10:2 FTOH (or an equivalent fluorotelomer derived precursor e.g. 8:2 FTA and 10:2 FTA). For TFA:PFPrA and PFBA:PFPeA, their ratios were always >2.8, suggesting

Table 1
Spearman correlation coefficients (r) and statistical significance (p) for $C_2 - C_{11}$ PFCAs. Strong correlations ($r > 0.70$) and statistically significant p-values are in bold ($p < 0.01$). More compounds are presented in Table S13.

	TFA	PFPrA	PFBA	PFPeA	PFHxA	PFHpA	PFOA	PFNA	PFDA
PFPrA	$r = 0.27$								
	$p = 0.30$								
PFBA	$r = 0.46$	$\mathbf{r = 0.91}$							
	$p = 0.06$	$\mathbf{p < 0.01}$							
PFPeA	$r = 0.39$	$\mathbf{r = 0.91}$	$\mathbf{r = 0.99}$						
	$p = 0.12$	$\mathbf{p < 0.01}$	$\mathbf{p < 0.01}$						
PFHxA	$r = 0.52$	$\mathbf{r = 0.87}$	$\mathbf{r = 0.97}$	$\mathbf{r = 0.97}$					
	p = 0.03	$\mathbf{p < 0.01}$	$\mathbf{p < 0.01}$	$\mathbf{p < 0.01}$					
PFHpA	$r = 0.34$	$r = 0.20$	$r = 0.40$	$r = 0.43$	r = 0.51				
	$p = 0.18$	$p = 0.43$	$p = 0.11$	$p = 0.08$	p = 0.03				
PFOA	$r = 0.50$	$r = 0.55$	$\mathbf{r = 0.72}$	$r = 0.68$	$\mathbf{r = 0.77}$	$r = 0.69$			
	p = 0.04	p = 0.02	$\mathbf{p < 0.01}$	$\mathbf{p < 0.01}$	$\mathbf{p < 0.01}$	$\mathbf{p < 0.01}$			
PFNA	$r = 0.08$	$r = 0.53$	$r = 0.51$	r = 0.53	$r = 0.54$	r = 0.52	$\mathbf{r = 0.77}$		
	$p = 0.76$	$p = 0.03$	p = 0.04	p = 0.03	$p = 0.02$	p = 0.03	$\mathbf{p < 0.01}$		
PFDA	$r = 0.06$	$r = 0.57$	$r = 0.51$	r = 0.54	$r = 0.53$	$r = 0.49$	$r = 0.67$	$\mathbf{r = 0.94}$	
	$p = 0.82$	p = 0.02	$p = 0.04$	p = 0.02	$p = 0.03$	$p = 0.05$	$\mathbf{p < 0.01}$	$\mathbf{p < 0.01}$	
PFUnDA	$r = -0.14$	$r = 0.44$	$r = 0.39$	$r = 0.45$	$r = 0.42$	$r = 0.51$	$r = 0.56$	$\mathbf{r = 0.83}$	$\mathbf{r = 0.89}$
	$p = 0.58$	p = 0.08	p = 0.12	$p = 0.07$	$p = 0.09$	p = 0.03	$p = 0.02$	$\mathbf{p < 0.01}$	$\mathbf{p < 0.01}$

an alternative major precursor source (or otherwise). It is worth noting that this approach relies on the assumption that branched PFCA isomers are insignificant to the levels of PFCAs found on Lomonosovfonna. This study has only been able to quantify linear isomers of PFCAs and therefore does not account for possible branched PFCA isomers. However, the analysis of surface water in two Arctic lakes in Canada found 99 % of PFOA was the linear isomer (De Silva et al., 2009). This suggests a fluorotelomer derived source since the PFAS manufacture by fluorotelomerization largely produces just linear isomers (Benskin et al., 2010). Since atmospheric precursors in the Arctic are known to be dominated by precursors manufactured by fluorotelomerization (Cai et al., 2012; Dreyer et al., 2009; Shoeib et al., 2006; Stock et al., 2007; Xie et al., 2015), it is expected that their PFCA degradation products will be largely linear isomers. Further work to establish the structural isomer profile of $C_8 - C_{11}$ PFCAs on Lomonosovfonna could assist with assigning 8:2 FTOH and 10:2 FTOH as precursor sources.

The higher total molar quantity of PFNA compared to PFOA in the ice core (0.81:1) indicates a preference for the formation of PFNA over PFOA (Figs. 2 and 3). This was also observed in the laboratory study of the degradation of 8:2 FTOH (0.94:1 molar ratio) by Ellis et al. (2004). Despite the numerous PFAS produced which could act as C8 atmospheric precursors (e.g. FASAs/FASEs), the slightly higher molar quantity of PFNA in the ice core over PFOA, indicates a stronger presence of a precursor(s) source that can degrade to both C8 and C9 PFCAs (i.e. 8:2 FTOH). This evidence, combined with the molar concentration ratios for PFOA:PFNA observed in this ice core, and other Arctic snow pits and ice cores (Young et al., 2007; Pickard et al., 2018; MacInnis et al., 2017), as well as widespread detection of 8:2 FTOH in the Arctic atmosphere (Cai et al., 2012; Dreyer et al., 2009; Shoeib et al., 2006; Stock et al., 2007; Xie et al., 2015), indicates that 8:2 FTOH continues to be a significant atmospheric source of PFOA and PFNA to the remote Arctic environment.

The PFCA homologue ratios for PFHxA:PFHpA, PFOA:PFNA, PFDA:PFUnDA at the Longyearbyen landfill (2.6, 3.8 and 4.2, respectively) and the Longyearbyen firefighting training site (3.3, 9.7 and < LOQ, respectively) (Ali et al., 2021) were in contrast to the results from the Lomonosovfonna ice core in this study (1.5, 0.81 and 0.93 respectively). This suggests that the input of PFAS to Lomonosovfonna from local sources in Longyearbyen is insignificant. This is likely due to the large distance (79 km) between Longyearbyen and Lomonosovfonna (which inhibits

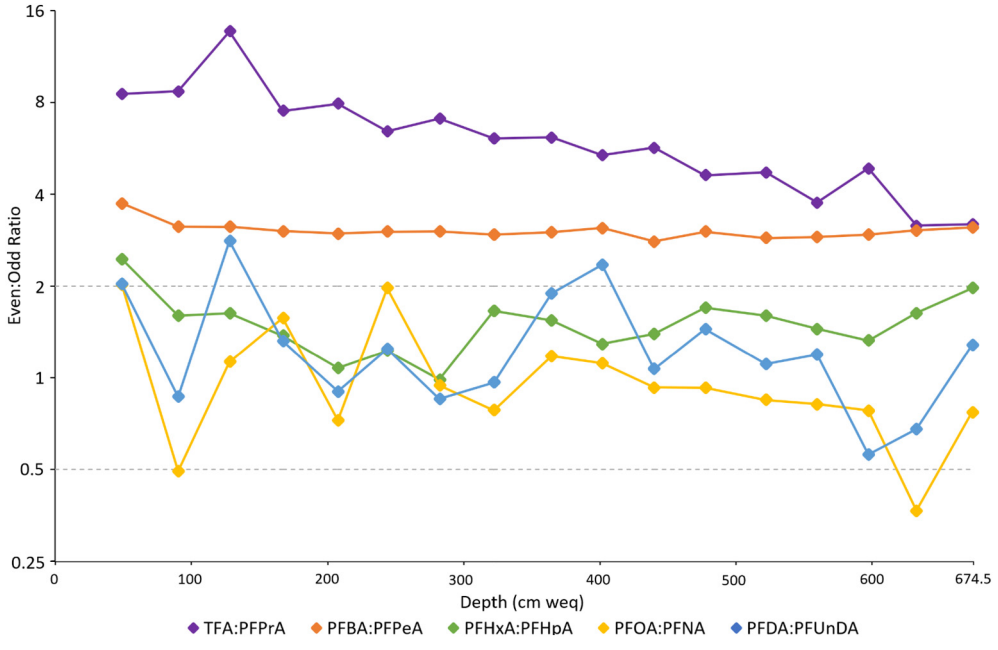

Fig. 3. Even:Odd molar concentration ratios for $C_2 - C_{11}$ PFCAs as a function of depth (cm weq).

direct transport), and the high elevation of Lomonosovfonna (1198 m.a.s.l.) above the tropospheric boundary layer (which atmospherically isolates Lomonosovfonna from local sources) (Garmash et al., 2013). It is worth noting that these even-odd PFCA homologues calculated from the Lomonosovfonna ice core (this study) and samples from Longyearbyen (Ali et al., 2021) are based on measurements of linear isomers alone. Although not confirmed, it is expected that sites in Longyearbyen will also be influenced by branched PFCA isomers, which are known to be present in aqueous firefighting foams (Kärrman et al., 2011). Despite this, linear PFCA homologue ratios suggest that known local PFAS emissions in Longyearbyen are not a source to Lomonosovfonna. Pyramiden is closer to Lomonosovfonna (31 km) and could be a potential local source of PFAS to the ice core. However, the settlement has been largely abandoned since 1998 (i.e. before the timespan of this ice core). Furthermore, Warner et al. (2019) found that PFAS in snow bunting (*Plectrophenax nivealis*) eggs had significantly lower levels in Pyramiden compared to Longyearbyen. No local sources were identified and long-range sources such as FTOHs were thought to be a more important exposure route for snow buntings in Pyramiden. Hence, Pyramiden does not provide a local source of PFAS to Lomonosovfonna, and the ice core in this study records an atmospheric record representative of a background location in the Arctic.

On Lomonosovfonna, the detection of 6:2 FTUCA (35 % > MQL) and 8:2 FTUCA (6 % > MQL) is further indicative of the FTOH degradation process (Ellis et al., 2004; Styler et al., 2013). During the radical-mediated degradation of 8:2 FTOH, it was found by Ellis et al. that 26 % of the molar reaction product would be 8:2 fluorotelomer acid (8:2 FTCA) (Ellis et al., 2004). The study reported that only the n:2 FTOH could yield the corresponding n:2 FTCA. Hence, the detection of FTUCAs in this ice core suggests that FTCAs have formed in the atmosphere. This is because any FTCAs formed will likely eliminate HF to form FTUCAs (Dinglasan et al., 2004; Loewen et al., 2005). This elimination process could happen in the environment (e.g. during snowpack/firn processes) or during extraction/analysis (e.g. during the preparation of the extracts in methanol). Regardless, the detection of 6:2 FTUCA and 8:2 FTUCA suggests that 6:2 FTOH and 8:2 FTOH provide atmospheric sources of PFCAs and other PFAS degradation products to the remote Arctic.

There was a significant correlation between all $C_3 - C_6$ PFCAs ($r > 0.87$, $p < 0.01$), but not TFA. This suggests a common chemical source or degradation pathway for $C_3 - C_6$ PFCAs. However, even-odd homologue ratios for $C_3 - C_5$ PFCAs do not suggest a fluorotelomer derived source (Fig. 3). Furthermore, the large variations in the PFCA mass contributions of PFPrA (16 %), PFBA (6 %), PFPeA (2 %), and PFHxA (1 %) in the ice core, and the higher fluxes of these PFCAs compared to $C_8 - C_{11}$ PFCAs, suggest a largely non-fluorotelomer derived source has contributed to their deposition (i.e. not FTOHs). The atmospheric deposition of PFPrA and PFBA are known to vary seasonally in the Arctic (Björnsdotter et al., 2021). This is because the photochemical conditions required for the radical-mediated degradation of C_3 and C_4 precursors were only found to exist during months with 24-hour daylight when solar radiation creates the atmospheric conditions for precursor degradation. Hence in this ice core, it is likely that PFPrA and PFBA, and by extension also PFPeA and PFHxA, have been formed during photochemical atmospheric conditions. A snowpit measured for PFAS on the Devon Ice Cap suggested that several non-fluorotelomer atmospheric sources for PFBA could for example include C_4 HFCs and HFEs, such as HFC-329 ($CF_3(CF_2)_3H$), HFE-7100 ($C_4F_9OCH_3$) and HFE-7200 ($C_4F_9OC_2H_5$) (MacInnis et al., 2017). These CFC replacement products, as well as other HFCs, HCFCs, HFEs and HFOs, provide an alternative atmospheric precursor source for short-chain PFCAs (Young et al., 2009a; Wallington et al., 1994; Oyaro et al., 2005; Young et al., 2009b; Montzka et al., 2015). These four precursor groups are known to exist in the atmosphere and are known to undergo a OH radical oxidation to PFCAs. Indeed, HFCs can provide a non-fluorotelomer precursor source for PFCAs of chain lengths greater than C_4. For example, HFC precursors could include HFC-52-13p ($CF_3(CF_2)_4CHF_2$, commercialized as AC-2000 or TH-6) for PFHxA (C_6) and HFC-569mccf ($CF_3(CF_2)_3CH_2CH_3$, commercialized as AC-4000 or TEH-4) for PFPeA (C_5) (Wang et al., 2014). Indeed, the tropospheric lifetime of HFC-52-13p is 31 years, which is sufficient to be well distributed in the atmosphere globally (Chen et al., 2004). Finally, the lack of correlation between TFA and other PFCAs could be due to a different precursor source profile for TFA. Indeed, TFA is the potential degradation product of over 1 million chemicals (Solomon et al., 2016).

3.3. Chemical sources of PFSAs to Lomonosovfonna

Observations of PFSAs were dominated by even chain length PFSAs over odd chain length PFSAs. For $C_2 - C_{10}$ PFSAs, PFPeS was only found in one subsection and was the only odd chain length PFSA detected. In contrast, PFBS, PFHxS, and PFOS were detected in 24 %, 65 %, and 82 % of subsections, respectively.

This study also quantified linear and perfluoromethyl branched isomers of PFHxS and PFOS. Inspecting the structural isomer profile is a useful tool in assigning sources of PFAS (Kärrman et al., 2007). In addition to linear-PFHxS and linear-PFOS, several other structural isomers were targeted. Similar MQLs for linear-PFHxS (4.4 pg L^{-1}) and linear-PFOS (6.6 pg L^{-1}), and their perfluoromethyl isomers (all 2.3 pg L^{-1}) remove possible biases in calculations due to large variations in MQLs. A summary of the concentrations of linear and branched isomers of PFHxS and PFOS can be found in Tables S14 and S15. Targeted branched isomers of PFHxS were only detected in one section of the core (6 % > MQL). In comparison, linear-PFHxS was detected in 65 % of core sections, but the concentrations were close to the MQL. This will discriminate against the less abundant branched isomers of PFHxS, which, if present on Lomonosovfonna, would be below the MQL. PFHxS, produced by electrochemical fluorination (ECF), has been reported to consist of approximately 18 % branched isomers (Benskin et al., 2010). In contrast, PFOS branched isomers were detected in 71 % of core subsections. 1-CF_3-PFOS was not detected, however at least one isomer of 3/4/5-CF_3-PFOS and one isomer of 6/2-CF_3-PFOS was detected. In core sections that detected both linear and branched isomers of PFOS, 71–89 % (average 81 %) were linear isomers. These results are similar to a standard PFOS product (76–79 %) produced by ECF (Kärrman et al., 2007). This suggests that changes to the PFOS isomer composition during transport to Lomonosovfonna are insignificant and therefore a direct particle-bound long-range atmospheric transport from Eurasian sources might explain the presence of PFOS on Lomonosovfonna. Two recent studies have found the percentage of PFOS in the atmosphere to be largely in the particle-bound phase at a background site in Europe (80 %) and in oceanic air from the Western Taiwan Strait (96 %) (Paragot et al., 2020; Yamazaki et al., 2021). Alternatively the presence of branched PFOS isomers could suggest a branched precursor source, such as branched FOSA precursors (Liu et al., 2007). In comparison to PFCAs, there is less evidence for precursors to act as an atmospheric source for PFSAs. Only one study has tenuously observed the formation of PFBS from *N*-methyl perfluorobutane sulfonamidoethanol (MeFBSE) in a simulated atmospheric laboratory study (D'eon et al., 2006). Hence in the atmosphere, the formation of PFSAs could proceed from the cleavage of S—N bonds in precursors such as FASAs and FASEs, which are known to be present in the Arctic atmosphere (Cai et al., 2012). In this ice core, PFOS was found to be significantly correlated with TFA ($r = 0.76$, $p < 0.01$). This could suggest that PFOS atmospheric formation and deposition is highly seasonally and dependent on the presence of OH radicals to enable the atmospheric degradation of PFOS precursors, as is the case for TFA (Björnsdotter et al., 2021). Further research is required to elucidate the significance of the direct particle-bound transport of PFSAs to the Arctic versus their atmospheric formation from precursors, or otherwise.

6:2 FTSA was detected in 41 % of subsections. Like for PFCAs, photochemical precursors also exist for 6:2 FTSA. These include 6:2 fluorotelomer sulfonamide alkylamine, 6:2 fluorotelomer sulfonamide alkylbetaine, and 6:2 fluorotelomer sulfonamide. These compounds have been found in the environment and are known to photochemically degrade to 6:2 FTSA (Moe et al., 2012; D'Agostino and Mabury, 2017a; D'Agostino and Mabury, 2017b). If some of these precursors, or others, would be sufficiently volatile to undergo long-range atmospheric transport to the Arctic, this could also explain the presence of 6:2 FTSA on Lomonosovfonna.

This study was unable to report TFMS concentrations. This is due to TFMS contamination introduced during the cutting and processing of the ice core in the cold lab (see *Quality Assurance and Quality Control*, pages S5 – S7). Nonetheless, Björnsdotter et al. (2021) recently reported the ubiquitous presence of TFMS in surface snow in the Arctic, including on Lomonosovfonna and other high elevation remote glaciers. However, this study was unable to assign a TFMS source. TFMS has not yet been targeted for a time series study in the Arctic, for example as part of atmospheric monitoring or an ice core. Such a study could help elucidate the source(s) of TFMS to the Arctic. Further work is required to assign the source(s) of TFMS in the Arctic.

3.4. Temporal trends in PFAS accumulation

Temporal trends show an increase in TFA atmospheric deposition (Fig. 4). This has also been observed in Germany and the Canadian Arctic (Pickard et al., 2020; Freeling et al., 2022). This likely reflects recent

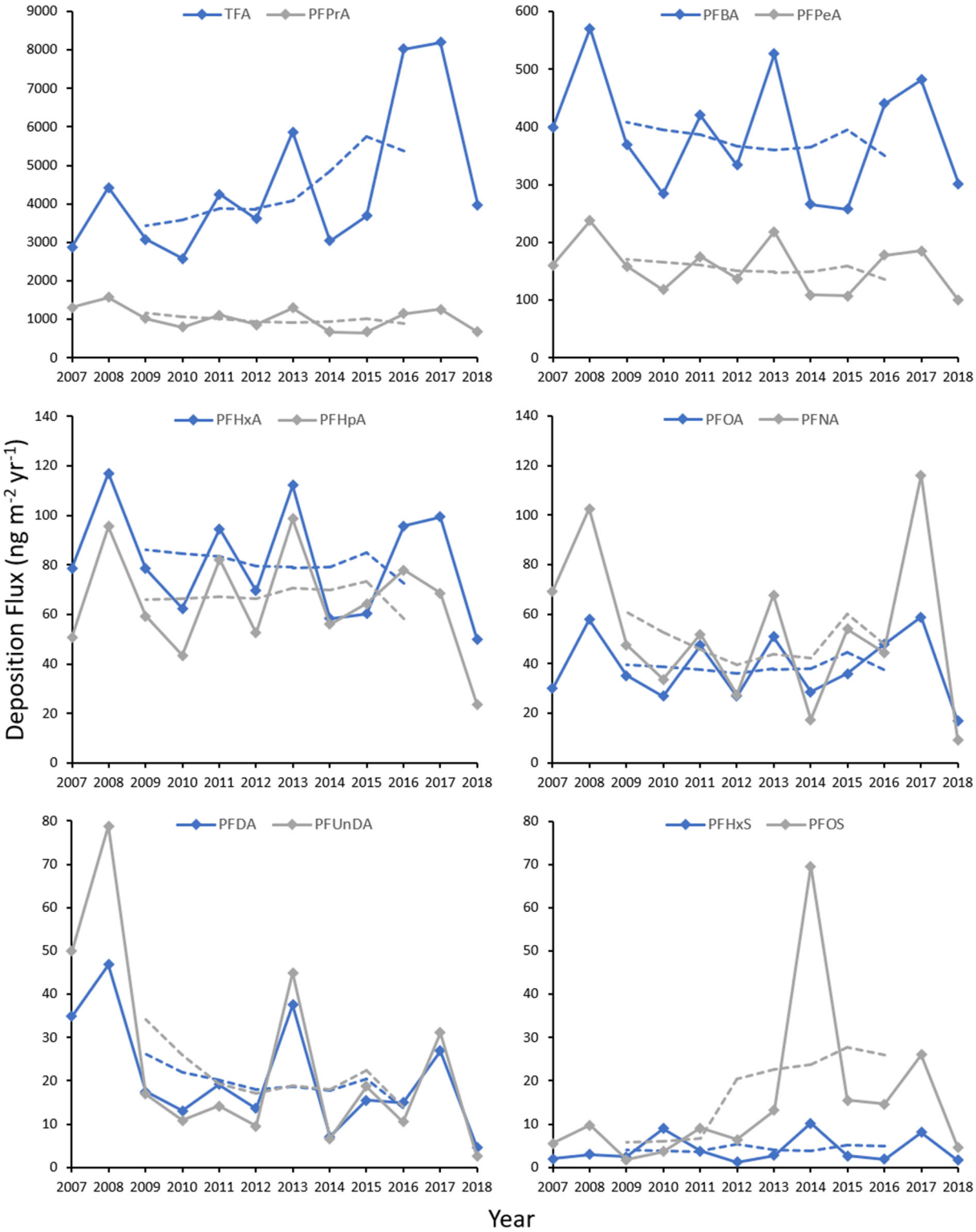

Fig. 4. Records of the annual atmospheric deposition fluxes of $C_2 - C_{11}$ PFCAs, PFHxS and PFOS. Solid line = annual deposition fluxes. Dashed line = 5-year moving average.

amendments to the Montreal Protocol that will see the replacement of HFCs with HFOs (Polonara et al., 2017). High deposition fluxes and increasing temporal trends for TFA mean that limited knowledge about the safe levels of TFA in the environment needs addressing. C_3 – C_9 PFCAs and PFHxS show neither a significant increase or decrease, whereas PFDA and PFUnDA show a decreasing trend in atmospheric deposition. This possibly reflects decreasing emissions of 10:2 FTOH precursors during 2010–2018 (Wang et al., 2014). PFOS however showed an increasing trend, particularly after 2011. This possibly suggests increasing atmospheric levels of PFOS precursors in the Arctic, however this is at odds with estimated decreasing emissions of FOSA, C_8 FASEs and their associated compounds (Wang et al., 2014).

No correlations were found between deposition fluxes of C_6 – C_{10} PFCAs, PFOS and FOSA on Lomonosovfonna and the atmospheric levels observed at the Zeppelin Observatory in Ny-Ålesund, Svalbard during the years 2007–2018 ($r < 0.17$, $p \geq 0.23$) (EBAS; Wong et al., 2021). This could be due to (i) differences in the measurement technique (Zeppelin only measures particle-bound PFAS, whereas photochemical degradation is likely gaseous) (Ellis et al., 2004; Sulbaek Andersen et al., 2005; Martin et al., 2006; D'eon et al., 2006; Butt et al., 2009), (ii) differences in geographic location (Svalbard is known to have an east-west gradient in climate) (Beaudon et al., 2013), (iii) PFAS mobility in the firn/snowpack during summer melt disrupting the atmospheric record, and (iv) disparity in air concentrations compared to atmospheric deposition. Indeed, one of the advantages of ice cores, compared to atmospheric measurements, is that it provides a record of what is deposited and can therefore enter the Arctic biosphere, compared to what is present in the air. The effects of melt percolation may also be significant in damaging the temporal trends in atmospheric deposition. To assist in overcoming this, a 5-year moving average was applied (see dashed lines in Fig. 4). The mobility of PFAS during meltwater percolation is discussed further in Section 3.7.

3.5. Marine environment as a source of PFAS

Several studies have identified marine aerosols as a potential mechanism for the long-range atmospheric transport of PFAS. For example, in a laboratory experiment, PFOA was found to be enriched in aerosols in the headspace above the parent water body (McMurdo et al., 2008). In another study, several particle-bound PFAAs were found to significantly correlate with marine aerosols in the atmosphere at two sites in Norway (Sha et al., 2022). Hence, marine aerosols could provide a mechanism for the transport of PFAS from the marine environment to Lomonosovfonna.

PFAS concentrations were investigated for correlations with Na^+ to investigate if marine aerosols were a source of PFAS to Lomonosovfonna (Table S16). Since Na^+ is expected to be entirely of a marine origin, Na^+ concentrations can be treated as a marine aerosol proxy. No PFAS were found to positively correlate with Na^+ ($r < 0.27$, $p > 0.30$). This indicates that marine aerosols are not a significant source for PFAS in the Lomonosovfonna ice core. This is despite (i) the ability of PFAS to undergo long-range transport in the ocean, (ii) the variety of PFAS that have been measured in the Arctic ocean (Yeung et al., 2017), and (iii) the proximity of Lomonosovfonna to several fjords (>20 km) and open sea (~120 km).

Several PFCAs and PFSAs have recently been found to significantly correlate with marine aerosols as part of long-term air monitoring at two sites in Norway (Sha et al., 2022). However, this study only considers the PFAS captured by quartz fiber filters and therefore only records particle-bound PFAS. So whilst particle-bound atmospheric PFAS may be linked to marine aerosols, the radical-mediated atmospheric degradation of PFAS precursors is likely a gaseous process (Ellis et al., 2004; Sulbaek Andersen et al., 2005; Martin et al., 2006; D'eon et al., 2006; Butt et al., 2009). Therefore, PFCAs and PFSAs formed by this process are likely not to have been captured by this study, or other long-term air monitoring which measure PFAS using filters alone. Unfortunately, few studies have measured both particle-bound and gaseous PFAAs in atmospheric samples (Paragot et al., 2020; Wong et al., 2018), and therefore the relative importance of each process is unclear.

3.6. Air mass source regions

Air mass trajectory frequency plots have previously been used to assist in assigning source regions for organic contaminants in ice cores (Garmash et al., 2013; Hermanson et al., 2010). In this study, 4383 daily trajectories from 2007 to 2018, were used to understand relevant air mass movements corresponding to the time period recorded by the ice core. This included one plot for all complete annual layers in the core (2007–2018, Fig. 5) and four further plots to investigate seasonal variations in air mass movements for these years (Fig. S2).

The overall plot shows the trajectory frequency for 2007–2018 based on a 6-day backward air mass trajectory from Lomonosovfonna. 0.25 % of trajectory endpoints passed over Arctic Canada, Greenland, Northern Europe, and Russia. Since Arctic Canada and Greenland are not highly populated or industrialized regions, this study suggests Eurasia as the main air mass source region to Lomonosovfonna. This would agree with previous contaminant records from Lomonosovfonna (Garmash et al., 2013; Osmont et al., 2018). A pollen record from Lomonosovfonna also identified Fennoscandia as a source and not North America (Hicks and Isaksson, 2006).

Seasonal plots showed increased trajectory frequency over Eurasia during November, December, and January, as well as February, March, and April (i.e. months with complete or partial darkness). During May, June, and July, trajectory densities over Eurasia were greatly reduced. Hence the direct long-range atmospheric transport of contaminants from Eurasian sources would likely be enhanced during winter months. This was also found to be the case during the seasonal air sampling of polycyclic aromatic hydrocarbons in Svalbard (Drotikova et al., 2021). This is in contrast to C_2 – C_4 PFCAs which were found to have higher deposition fluxes from precursor degradations during months with 24-hour daylight (Björnsdotter et al., 2021).

Using HYSPLIT to assign geographical source regions has been shown to be effective for organic contaminants such as polychlorinated biphenyls (PCBs) in ice cores (Garmash et al., 2013). If PFAS on Lomonosovfonna have been transported by direct emissions like PCBs, then these trajectory frequency plots are also a helpful tool in assigning source regions. However, many of the PFAS observed in this ice core, such as PFCAs, are likely formed by the atmospheric degradation of precursors. PFAS precursors have long atmospheric lifetimes with respect to radical degradation (e.g. FTOHs – 20 days, HFC-134a – 14.1 years) (Ellis et al., 2003; Wild et al., 1996). As a result, using HYSPLIT to assign geographical source regions is not possible. Since PFCAs have atmospheric lifetimes of several days with respect to wet and dry deposition (TFA – 9 days, PFOA – 12 days) (Wallington et al., 2006; Kotamarthi et al., 1998), trajectory frequency plots instead represent regions where degradation products, such as PFCAs, could have been formed in the atmosphere from precursors rather than source regions of PFAS precursors.

3.7. Redistribution of PFAS during melt

Iizuka et al. (2002) have established a chemical melt proxy using Na^+ and Mg^{2+} ion concentrations for Svalbard ice cores. This has been shown to be effective in recording historical melt for several Svalbard ice cores due to the preferential mobility of Mg^{2+} compared to Na^+ during meltwater percolation in the snowpack/firn. This study uses the same chemical melt proxy by calculating $\log([Na^+]/[Mg^{2+}])$ values.

PFAS are likely ubiquitous in seasonal snow and post-industrial accumulation on glaciers in Svalbard. For PFAS, post-industrial accumulation will be from approximately 1940 onwards, since it was during this decade that PFAS entered commercial production (Banks and Tatlow, 1986). Investigating the effects of meltwater percolation on the core could offer a route to understanding which PFAS are released preferentially during snowmelt and glacier runoff. This is important because runoff from glaciers could be a large seasonal source of PFAS to the fjord environment in Svalbard and the wider Arctic. PFCAs and PFSAs have high solubility and would be expected to be very mobile during events when meltwater percolates through the snowpack/firn (Rayne and Forest, 2009). Plassmann et al.

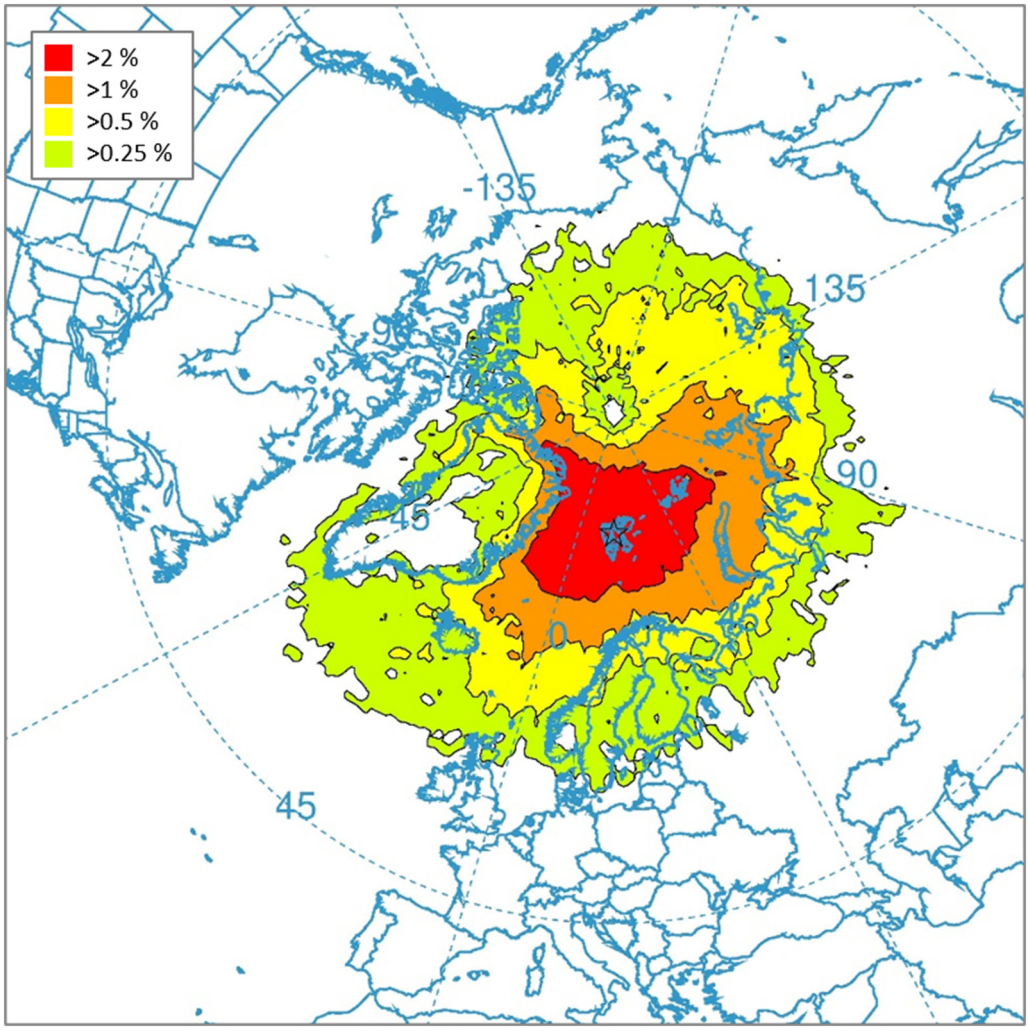

Fig. 5. HYSPLIT air mass trajectory frequency plot for air masses ending at the Lomonosovfonna drilling site 2007–2018.

(2011) investigated the influence of snowmelt on PFCAs and PFSAs in a snow chamber experiment and found that PFCAs and PFSAs of shorter chain lengths were preferentially eluted. Field observations broadly found the same results that shorter chain length PFCAs were more mobile during melt of the seasonal snowpack (Skaar et al., 2019; Codling et al., 2014). To assess whether PFAS concentrations had been affected by percolating meltwater, their correlations with the melt proxy log($[Na^+]/[Mg^{2+}]$) were investigated (Table S16). TFA ($r = -0.65, p < 0.01$) and PFOS ($r = -0.54, p = 0.02$) were found to have negative correlation with the melt proxy (i.e. TFA concentrations were lower in subsections where Mg^{2+} concentrations had been depleted relative to Na^+ as a result of meltwater percolation). This suggests that TFA, and possibly PFOS, are mobile during meltwater percolation through the snowpack/firn. Nonetheless, it is possible that other PFAS may have been affected by meltwater percolation due to their high water solubilities (Rayne and Forest, 2009). Hence, runoff from post-industrial accumulation on glaciers and seasonal snowmelt would be important in the seasonal input of TFA and PFOS, and possibly other PFAS, to the fjord environment in Svalbard and elsewhere in the Arctic.

Meltwater percolation of chemical species on Lomonosovfonna is well understood. In a previous ice core from Lomonosovfonna, one study found that meltwater was mostly refrozen within the annual layer (Pohjola et al., 2002), whereas another study found that percolation may have extended up to 8 annual layers (Moore et al., 2005). Regardless, these effects, combined with the short time period covered by the core (2006–2019) make it difficult to comment on the long-term trends in PFAS deposition fluxes in this ice core. Furthermore, this makes it challenging to assign geographical source regions for sections of the ice core which have higher individual PFAS fluxes. Meltwater percolation also damages the atmospheric signal from water stable isotopes and major ions. This can affect the accuracy of dating the ice core (and hence a ± 2 year error has been assigned to the annual layer counting, Fig. S1). Misassignment of annual layers could then affect the PFAS annual flux values reported in this study. Meltwater percolation in the snowpack/firn would also provide an alternative aqueous medium for degradations to occur. Indeed, the post-deposition degradation of PFAS precursors in the snowpack (i.e. any degradation which follows wet/dry deposition), in addition to atmospheric degradations, could affect the PFAAs observed in this study (Taniyasu et al., 2013). Several neutral PFAS are known to have positive and negative air-snow exchange fluxes, and therefore there can be post-deposition losses from the snowpack/firn back to the atmosphere (Xie et al., 2015). The analysis of this ice core is unable to distinguish between particle-bound PFAS and non-particle-bound PFAS, and hence reports a sum value. However, given the collective evidence for precursor sources for C_2 – C_{11} PFCAs, and since this is known that their degradation is a gaseous process, it is likely that at least these degradation products exist mostly as non-particle-bound compounds in the ice core.

3.8. Environmental implications

HYSPLIT analysis (Section 3.6) reveals a broad atmospheric region which has influenced the PFAS observed in this ice core. This area extends through northern Eurasia, Greenland, Canada and almost the entire Arctic

Ocean (Fig. 5). Hence, this study has been able understand atmospheric processes, including precursor degradations, occurring in a large part of the Arctic and northern Eurasian atmosphere. Results suggest that the atmospheric degradation of precursors (e.g. FTOHs, HFCs) are responsible for the presence of PFCAs on Lomonosovfonna and that their atmospheric deposition fluxes increase greatly towards shorter chain length PFCAs in several Arctic ice cores (Fig. 2). TFA was found to have the highest atmospheric deposition fluxes, and its temporal trends are now known to be increasing in both the European Arctic (Fig. 4) and Canadian Arctic (Pickard et al., 2020). The mobility of some PFAS, such as TFA, during meltwater percolation in this ice core suggests that increasing equilibrium-line altitudes on Arctic glaciers due to climate change (Van Pelt et al., 2019), may enhance the input of some PFAS to downstream Arctic ecosystems (e.g. Arctic fjords, lakes and wetlands) through glacier runoff.

4. Conclusion

The presence of 26 of the 45 PFAS targeted in a remote high elevation Arctic ice core suggest that PFAS contamination is chemically diverse and geographically widespread in the Arctic. The majority of PFAS frequently detected were PFCAs, and fluxes of PFCAs typically increased towards shorter chain lengths with TFA having the highest fluxes in the core. The distribution profile of PFAS detected suggests that FTOHs are likely the atmospheric precursor to $C_8 – C_{11}$ PFCAs, whereas $C_3 – C_6$ PFCAs have an alternative source, such as HFCs and other CFC replacement compounds. In addition, the detection of FTUCAs confirmed the role of FTOHs as atmospheric precursors to PFCAs. It is unclear whether the presence of PFSAs, such as PFBS, PFHxS, and PFOS, on Lomonosovfonna could be explained by direct particle-bound transport or atmospheric degradation of precursors. Nonetheless, the structural isomer profile of PFOS on Lomonosovfonna indicated that it had been manufactured by ECF. No PFAS were found to positively correlate with the Na^+, a marine aerosol proxy, showing that marine aerosols are unimportant in the atmospheric transport of PFAS to the Arctic. HYSPLIT analysis revealed that any direct transport of contaminants would come from Eurasian sources. TFA, and possibly also PFOS, were found to be influenced by meltwater percolation in the ice core, indicating the importance of glacier runoff as a seasonal source of PFAS input into Arctic fjords. In comparison with another Arctic ice core from the Devon Ice Cap (2007–2014), fluxes for C_2 and C_3 PFCAs were typically lower, but fluxes were similar or higher for $C_4 – C_{13}$ PFCAs and PFOS on Lomonosovfonna.

CRediT authorship contribution statement

William F. Hartz: Conceptualization, Methodology, Validation, Formal analysis, Investigation, Resources, Writing – original draft, Visualization, Project administration, Funding acquisition. **Maria K. Björnsdotter:** Conceptualization, Methodology, Validation, Formal analysis, Investigation, Resources, Writing – review & editing. **Leo W.Y. Yeung:** Conceptualization, Methodology, Validation, Formal analysis, Resources, Writing – review & editing, Supervision, Funding acquisition. **Andrew Hodson:** Resources, Writing – review & editing, Supervision, Project administration. **Elizabeth R. Thomas:** Formal analysis, Resources, Writing – review & editing, Supervision, Funding acquisition. **Jack D. Humby:** Methodology, Validation, Formal analysis, Investigation, Resources, Writing – review & editing. **Chris Day:** Methodology, Validation, Investigation, Resources, Writing – review & editing, Funding acquisition. **Ingrid Ericson Jogsten:** Resources, Writing – review & editing, Supervision, Funding acquisition. **Anna Kärrman:** Resources, Writing – review & editing, Supervision, Funding acquisition. **Roland Kallenborn:** Conceptualization, Resources, Writing – review & editing, Supervision, Project administration, Funding acquisition.

Data availability

All data is available in the Appendix

Declaration of competing interest

The authors declare that they have no known competing financial interests or personal relationships that could have appeared to influence the work reported in this paper.

Acknowledgements

The authors gratefully acknowledge financial support from the Swedish Research Council Formas (2016-01284), the United Kingdom Research and Innovation Natural Environment Research Council and the Oxford Doctoral Training Partnership in Environmental Research (NE/L002612/1), the Burdett-Coutts Trust, the Svalbard Science Forum Arctic Field Grant 2019 (RiS ID 11121), the Research Council of Norway (SvalPOP, 196218/S30), the Fram Centre Flagship program (PharmArctic, 534/75219) and the Knowledge Foundation (Enforce Research Project, 20160019). The authors would also like to thank the Logistics Department and colleagues at the University Centre in Svalbard for help organizing and assisting with fieldwork, and Veerle van Winden, Eirik Rolland Enger and Julien-Pooya Weihs for assistance in the field and laboratory. The authors also grateful acknowledge Pernilla Bohlin-Nizzetto for providing the Zeppelin monitoring data from the EBAS database.

Appendix A. Supporting information

Full details of the drill site characteristics, chemicals and reagents, sample extraction, instrument analysis, quality control and quality assurance, HYSPLIT analysis, major ion analysis, and water stable isotope analysis can be found in the supporting information (pages S1 – S9). Lists of target analytes, abbreviations, CAS numbers, MRM transitions, internal and recovery standards used, LODs and MQLs, extraction efficiencies and the repeatability of the instrument method can also be found. Tables with PFAS fluxes and concentrations, as well as correlations, are also provided. Figures showing annual layer counting used in dating the ice core, and HYSPLIT seasonal trajectory frequency plots can also be found. The supporting information to this article can be found online at https://doi.org/10.1016/j.scitotenv.2023.161830

References

Ali, A.M., et al., 2021. The fate of poly- and perfluoroalkyl substances in a marine food web influenced by land-based sources in the Norwegian Arctic. Environ. Sci. Process. Impacts 23, 588–604.
Banks, R.E., Tatlow, J.C., 1986. Synthesis of C-F bonds: the pioneering years, 1835–1940. J. Fluor. Chem. 33, 71–108.
Barbaro, E., et al., 2021. Measurement report: spatial variations in ionic chemistry and water-stable isotopes in the snowpack on glaciers across Svalbard during the 2015–2016 snow accumulation season. Atmos. Chem. Phys. 21, 3163–3180.
Beaudon, E., et al., 2013. Lomonosovfonna and Holtedahlfonna ice cores reveal east–west disparities of the Spitsbergen environment since AD 1700. J. Glaciol. 59, 1069–1083.
Benskin, J.P., De Silva, A.O., Martin, J.W., 2010. Isomer profiling of perfluorinated substances as a tool for source tracking: a review of early findings and future applications. Rev. Environ. Contam. Toxicol. 208, 111–160.
Benskin, J.P., et al., 2012. Perfluoroalkyl acids in the Atlantic and Canadian Arctic oceans. Environ. Sci. Technol. 46, 5815–5823.
Björnsdotter, M.K., et al., 2021. Levels and seasonal trends of C1–C4 perfluoroalkyl acids and the discovery of trifluoromethane sulfonic acid in surface snow in the Arctic. Environ. Sci. Technol. 55, 15853–15861.
Burgay, F., et al., 2021. First discrete iron(II) records from Dome C (Antarctica) and the Holtedahlfonna glacier (Svalbard). Chemosphere 267, 129335.
Butt, C.M., Young, C.J., Mabury, S.A., Hurley, M.D., Wallington, T.J., 2009. Atmospheric chemistry of 4:2 fluorotelomer acrylate [C4F9CH2CH2OC(O)CH═CH2]: kinetics, mechanisms, and products of chlorine-atom- and OH-radical-initiated oxidation. J. Phys. Chem. A 113, 3155–3161.
Cai, M., et al., 2012. Polyfluorinated compounds in the atmosphere along a cruise pathway from the Japan Sea to the Arctic Ocean. Chemosphere 87, 989–997.
Chen, L., Tokuhashi, K., Kutsuna, S., Sekiya, A., 2004. Rate constants for the gas-phase reaction of CF3CF2CF2CF2CF2CHF2 with OH radicals at 250–430 K. Int. J. Chem. Kinet. 36, 26–33.
Codling, G., et al., 2014. The fate of per- and polyfluoroalkyl substances within a melting snowpack of a boreal forest. Environ. Pollut. 191, 190–198.
Conder, J.M., Hoke, R.A., De Wolf, W., Russell, M.H., Buck, R.C., 2008. Are PFCAs bioaccumulative? A critical review and comparison with regulatory criteria and persistent lipophilic compounds. Environ. Sci. Technol. 42, 995–1003.

Cousins, I.T., Johansson, J.H., Salter, M.E., Sha, B., Scheringer, M., 2022. Outside the safe operating space of a new planetary boundary for per- and polyfluoroalkyl substances (PFAS). Environ. Sci. Technol. 56, 11172–11179.
D'Agostino, L.A., Mabury, S.A., 2017. Aerobic biodegradation of 2 fluorotelomer sulfonamide–based aqueous film–forming foam components produces perfluoroalkyl carboxylates. Environ. Toxicol. Chem. 36, 2012–2021.
D'Agostino, L.A., Mabury, S.A., 2017. Certain perfluoroalkyl and polyfluoroalkyl substances associated with aqueous film forming foam are widespread in Canadian surface waters. Environ. Sci. Technol. 51, 13603–13613.
D'eon, J.C., Hurley, M.D., Wallington, T.J., Mabury, S.A., 2006. Atmospheric chemistry of N-methyl perfluorobutane sulfonamidoethanol, C4F9SO2N(CH3)CH2CH2OH: kinetics and mechanism of reaction with OH. Environ. Sci. Technol. 40, 1862–1868.
De Silva, A.O., Muir, D.C.G., Mabury, S.A., 2009. Distribution of perfluorocarboxylate isomers in select samples from the North American environment. Environ. Toxicol. Chem. 28, 1801–1814.
Dinglasan, M.J.A., Ye, Y., Edwards, E.A., Mabury, S.A., 2004. Fluorotelomer alcohol biodegradation yields poly- and perfluorinated acids. Environ. Sci. Technol. 38, 2857–2864.
Dreyer, A., Weinberg, I., Temme, C., Ebinghaus, R., 2009. Polyfluorinated compounds in the atmosphere of the Atlantic and southern oceans: evidence for a global distribution. Environ. Sci. Technol. 43, 6507–6514.
Drotikova, T., Dekhtyareva, A., Kallenborn, R., Albinet, A., 2021. Polycyclic aromatic hydrocarbons (PAHs) and their nitrated and oxygenated derivatives in the Arctic boundary layer: seasonal trends and local anthropogenic influence. Atmos. Chem. Phys. 21.
EBAS, .. https://ebas.nilu.no/.
Ellis, D.A., et al., 2003. Atmospheric lifetime of fluorotelomer alcohols. Environ. Sci. Technol. 37, 3816–3820.
Ellis, D.A., et al., 2004. Degradation of fluorotelomer alcohols: a likely atmospheric source of perfluorinated carboxylic acids. Environ. Sci. Technol. 38, 3316–3321.
Freeling, F., et al., 2022. Levels and temporal trends of trifluoroacetate (TFA) in archived plants: evidence for increasing emissions of gaseous TFA precursors over the last decades. Environ. Sci. Technol. Lett. 9, 400–405.
Frömel, T., Knepper, T.P., 2010. Biodegradation of fluorinated alkyl substances. Rev. Environ. Contam. Toxicol. 208, 161–177.
Garmash, O., et al., 2013. Deposition history of polychlorinated biphenyls to the Lomonosovfonna glacier, Svalbard: a 209 congener analysis. Environ. Sci. Technol. 47, 12064–12072.
Hermanson, M.H., et al., 2010. Deposition history of brominated flame retardant compounds in an ice core from Holtedahlfonna, Svalbard,Norway. Environ. Sci. Technol. 44, 7405–7410.
Hicks, S., Isaksson, E., 2006. Assessing source areas of pollutants from studies of fly ash, charcoal, and pollen from Svalbard snow and ice. J. Geophys. Res. Atmos. 111.
Iizuka, Y., Igarashi, M., Kamiyama, K., Motoyama, H., Watanabe, O., 2002. Ratios of Mg2+/Na+ in snowpack and an ice core at Austfonna ice cap, Svalbard, as an indicator of seasonal melting. J. Glaciol. 48, 452–460.
Isaksson, E., et al., 2003. Ice cores from Svalbard—useful archives of past climate and pollution history. Phys. Chem. EarthA/B/C 28, 1217–1228.
ISO 25101:2009, 2009. Water quality — determination of perfluorooctanesulfonate (PFOS) and perfluorooctanoate (PFOA) — method for unfiltered samples using solid phase extraction and liquid chromatography/mass spectrometry. https://www.iso.org/standard/42742.html.
Jensen, A.A., Leffers, H., 2008. Emerging endocrine disrupters: perfluoroalkylated substances. Int. J. Androl. 31, 161–169.
Karasiński, G., et al., 2014. Lidar observations of volcanic dust over Polish Polar Station at Hornsund after eruptions of Eyjafjallajökull and Grímsvötn. Acta Geophys. 62, 316–339.
Kärrman, A., Langlois, I., van Bavel, B., Lindström, G., Oehme, M., 2007. Identification and pattern of perfluorooctane sulfonate (PFOS) isomers in human serum and plasma. Environ. Int. 33, 782–788.
Kärrman, A., Elgh-Dalgren, K., Lafossas, C., Møskeland, T., 2011. Environmental levels and distribution of structural isomers of perfluoroalkyl acids after aqueous fire-fighting foam (AFFF) contamination. Environ. Chem. 8, 372–380.
Kotamarthi, V.R., et al., 1998. Trifluoroacetic acid from degradation of HCFCs and HFCs: a three-dimensional modeling study. J. Geophys. Res. Atmos. 103, 5747–5758.
Kwok, K.Y., et al., 2013. Transport of perfluoroalkyl substances (PFAS) from an arctic glacier to downstream locations: implications for sources. Sci. Total Environ. 447, 46–55.
Kwok, K.Y., et al., 2013. Transport of perfluoroalkyl substances (PFAS) from an arctic glacier to downstream locations: implications for sources. Sci. Total Environ. 447, 46–55.
Liu, P., et al., 2007. Theoretical studies of the conformations and 19F NMR spectra of linear and a branched perfluorooctanesulfonamide (PFOSAmide). Chemosphere 69, 1213–1220.
Loewen, M., Halldorson, T., Wang, F., Tomy, G., 2005. Fluorotelomer carboxylic acids and PFOS in rainwater from an urban center in Canada. Environ. Sci. Technol. 39, 2944–2951.
MacInnis, J.J., et al., 2017. Emerging investigator series: a 14-year depositional ice record of perfluoroalkyl substances in the High Arctic. Environ. Sci. Process. Impacts 19, 22–30.
Martin, J.W., Ellis, D.A., Mabury, S.A., Hurley, M.D., Wallington, T.J., 2006. Atmospheric chemistry of perfluoroalkanesulfonamides: kinetic and product studies of the OH radical and Cl atom initiated oxidation of N-ethyl perfluorobutanesulfonamide. Environ. Sci. Technol. 40, 864–872.
McMurdo, C.J., et al., 2008. Aerosol enrichment of the surfactant PFO and mediation of the water–air transport of gaseous PFOA. Environ. Sci. Technol. 42, 3969–3974.
Moe, M.K., et al., 2012. The structure of the fire fighting foam surfactant Forafac®1157 and its biological and photolytic transformation products. Chemosphere 89, 869–875.
Montzka, S.A., et al., 2015. Recent trends in global emissions of hydrochlorofluorocarbons and hydrofluorocarbons: reflecting on the 2007 adjustments to the Montreal protocol. J. Phys. Chem. A 119, 4439–4449.
Moore, J.C., Grinsted, A., Kekonen, T., Pohjola, V., 2005. Separation of melting and environmental signals in an ice core with seasonal melt. Geophys. Res. Lett. 32, 1–4.
Muir, D., et al., 2019. Levels and trends of poly- and perfluoroalkyl substances in the Arctic environment – an update. Emerg. Contam. 5, 240–271.
Osmont, D., et al., 2018. An 800-year high-resolution black carbon ice core record from Lomonosovfonna,Svalbard. Atmos. Chem. Phys. 18, 12777–12795.
Oyaro, N., Sellevåg, S.R., Nielsen, C.J., 2005. Atmospheric chemistry of hydrofluoroethers: reaction of a series of hydrofluoroethers with OH radicals and Cl atoms, atmospheric lifetimes, and global warming potentials. J. Phys. Chem. A 109, 337–346.
Paragot, N., et al., 2020. Multi-year atmospheric concentrations of per- and polyfluoroalkyl substances (PFASs) at a background site in central Europe. Environ. Pollut. 265, 114851.
Pickard, H.M., et al., 2018. Continuous non-marine inputs of per- and polyfluoroalkyl substances to the High Arctic: a multi-decadal temporal record. Atmos. Chem. Phys. 18, 5045–5058.
Pickard, H.M., et al., 2020. Ice core record of persistent short-chain fluorinated alkyl acids: evidence of the impact from global environmental regulations. Geophys. Res. Lett. 47.
Pike, K.A., Edmiston, P.L., Morrison, J.J., Faust, J.A., 2021. Correlation analysis of perfluoroalkyl substances in regional U.S. precipitation events. Water Res. 190, 116685.
Plassmann, M.M., et al., 2011. Laboratory studies on the fate of perfluoroalkyl carboxylates and sulfonates during snowmelt. Environ. Sci. Technol 45, 6872–6878.
Pohjola, V.A., et al., 2002. Effect of periodic melting on geochemical and isotopic signals in an ice core from Lomonosovfonna,Svalbard. J. Geophys. Res. 107, 4036.
Polonara, F., Kuijpers, L.J.M., Peixoto, R.A., 2017. Potential impacts of the Montreal Protocol Kigali Amendment to the choice of refrigerant alternatives. Int. J. Heat Technol. 35, S1–S8.
Rayne, S., Forest, K., 2009. Perfluoroalkyl sulfonic and carboxylic acids: a critical review of physicochemical properties, levels and patterns in waters and wastewaters, and treatment methods. J. Environ. Sci. Health A 44, 1145–1199.
Sha, B., et al., 2022. Sea spray aerosol (SSA) as a source of perfluoroalkyl acids (PFAAs) to the atmosphere: field evidence from long-term air monitoring. Environ. Sci. Technol. 56, 228–238.
Shoeib, M., Harner, T., Vlahos, P., 2006. Perfluorinated chemicals in the arctic atmosphere. Environ. Sci. Technol. 40, 7577–7583.
Skaar, J.S., Ræder, E.M., Lyche, J.L., Ahrens, L., Kallenborn, R., 2019. Elucidation of contamination sources for poly- and perfluoroalkyl substances (PFASs) on Svalbard (Norwegian Arctic). Environ. Sci. Pollut. Res. 26, 7356–7363.
Solomon, K.R., et al., 2016. Sources, fates, toxicity, and risks of trifluoroacetic acid and its salts: relevance to substances regulated under the Montreal and Kyoto protocols. J. Toxicol. Environ. Health B Crit. Rev. 19, 289–304.
Stock, N.L., Furdui, V.I., Muir, D.C.G., Mabury, S.A., 2007. Perfluoroalkyl contaminants in the Canadian Arctic: evidence of atmospheric transport and local contamination. Environ. Sci. Technol. 41, 3529–3536.
Styler, S.A., Myers, A.L., Donaldson, D.J., 2013. Heterogeneous photooxidation of fluorotelomer alcohols: a new source of aerosol-phase perfluorinated carboxylic acids. Environ. Sci. Technol. 47, 6358–6367.
Sulbaek Andersen, M.P., et al., 2005. Atmospheric chemistry of 4:2 fluorotelomer alcohol (n-C4F9CH2CH2OH): products and mechanism of Cl atom initiated oxidation in the presence of NO x. J. Phys. Chem. A 109, 1849–1856.
Taniyasu, S., et al., 2013. Does wet precipitation represent local and regional atmospheric transportation by perfluorinated alkyl substances? Environ. Int. 55, 25–32.
Van Pelt, W., et al., 2019. A long-term dataset of climatic mass balance, snow conditions, and runoff in Svalbard (1957–2018). Cryosphere 13, 2259–2280.
Velders, G.J.M., Andersen, S.O., Daniel, J.S., Fahey, D.W., McFarland, M., 2007. The importance of the Montreal Protocol in protecting climate. Proc. Natl. Acad. Sci. U. S. A. 104, 4814–4819.
Wallington, T.J., et al., 1994. The environmental impact of CFC replacements-HFCs and HCFCs. Environ. Sci. Technol. 28.
Wallington, T.J., et al., 2006. Formation of C7F15COOH (PFOA) and other perfluorocarboxylic acids during the atmospheric oxidation of 8:2 fluorotelomer alcohol. Environ. Sci. Technol. 40, 924–930.
Wang, Z., Cousins, I.T., Scheringer, M., Buck, R.C., Hungerbühler, K., 2014. Global emission inventories for C4–C14 perfluoroalkyl carboxylic acid (PFCA) homologues from 1951 to 2030, part II: the remaining pieces of the puzzle. Environ. Int. 69, 166–176.
Wang, X., Chen, M., Gong, P., Wang, C., 2019. Perfluorinated alkyl substances in snow as an atmospheric tracer for tracking the interactions between westerly winds and the Indian Monsoon over western China. Environ. Int. 124, 294–301.
Wang, Z., et al., 2021. A new OECD definition for per- and polyfluoroalkyl substances. Environ. Sci. Technol. 55, 15575–15578.
Warner, N.A., et al., 2019. Snow buntings (Plectrophenax nivalis) as bio-indicators for exposure differences to legacy and emerging persistent organic pollutants from the Arctic terrestrial environment on Svalbard. Sci. Total Environ. 667, 638–647.
Wickström, S., Jonassen, M.O., Cassano, J.J., Vihma, T., 2020. Present temperature, precipitation, and rain-on-snow climate in Svalbard. J. Geophys. Res. Atmos. 125, e2019JD032155.
Wild, O., Ratfigan, O.V., Jones, R.L., Pyle, J.A., Cox, R.A., 1996. Two-dimensional modelling of some CFC replacement compounds. J. Atmos. Chem. 25, 167.
Wong, F., et al., 2018. Assessing temporal trends and source regions of per- and polyfluoroalkyl substances (PFASs) in air under the Arctic Monitoring and Assessment Programme (AMAP). Atmos. Environ. 172, 65–73.
Wong, F., et al., 2021. Time trends of persistent organic pollutants (POPs) and Chemicals of Emerging Arctic Concern (CEAC) in Arctic air from 25 years of monitoring. Sci. Total Environ. 775.
Xie, Z., et al., 2015. Neutral poly-/perfluoroalkyl substances in air and snow from the Arctic. Sci. Rep. 5, 8912.
Yamazaki, E., Taniyasu, S., Wang, X., Yamashita, N., 2021. Per- and polyfluoroalkyl substances in surface water, gas and particle in open ocean and coastal environment. Chemosphere 272, 129869.
Yde, J.C., Riger-Kusk, M., Christiansen, H.H., Knudsen, N.T., Humlum, O., 2008. Hydrochemical characteristics of bulk meltwater from an entire ablation season, Longyearbreen,Svalbard. J. Glaciol. 54, 259–272.

Yeung, L.W., et al., 2017. Vertical profiles, sources, and transport of PFASs in the Arctic Ocean. Environ. Sci. Technol. 51, 6735–6744.
Young, C.J., et al., 2007. Perfluorinated acids in Arctic snow: new evidence for atmospheric formation. Environ. Sci. Technol. 41, 3455–3461.
Young, C.J., Hurley, M.D., Wallington, T.J., Mabury, S.A., 2009. Atmospheric chemistry of CF3CF2H and CF3CF2CF2CF2H: kinetics and products of gas-phase reactions with cl atoms and OH radicals, infrared spectra, and formation of perfluorocarboxylic acids. Chem. Phys. Lett. 473, 251–256.
Young, C.J., Hurley, M.D., Wallington, T.J., Mabury, S.A., 2009. Atmospheric chemistry of perfluorobutenes (CF3CF = CFCF3 and CF3CF2CF = CF2): kinetics and mechanisms of reactions with OH radicals and chlorine atoms, IR spectra, global warming potentials, and oxidation to perfluorocarboxylic acids. Atmos. Environ. 43, 3717–3724.